

Supplementary Information for

**Phosphorescent organoplatinum(II) complexes with a lipophilic anion: Supramolecular soft nanomaterials through ionic self-assembly and metallophilicity**

Yong Chen,<sup>a,b</sup> Chi-Ming Che<sup>\*a</sup> and Wei Lu<sup>\*c</sup>

<sup>a</sup> State Key Laboratory of Synthetic Chemistry, HKU-CAS Joint Laboratory on New Materials, and Department of Chemistry, The University of Hong Kong, Pokfulam Road, Hong Kong, P. R. China. Email: cmche@hku.hk

<sup>b</sup> Key Laboratory of Photochemical Conversion and Optoelectronic Materials, Technical Institute of Physics and Chemistry, Chinese Academy of Sciences, Beijing 100190, P. R. China.

<sup>c</sup> Department of Chemistry, South University of Science and Technology of China, Shenzhen, Guangdong 518055, P. R. China. Email: luw@sustc.edu.cn

Characterization data and supplementary photophysical data, diffractograms, and thermograms.

## **Experimental Section:**

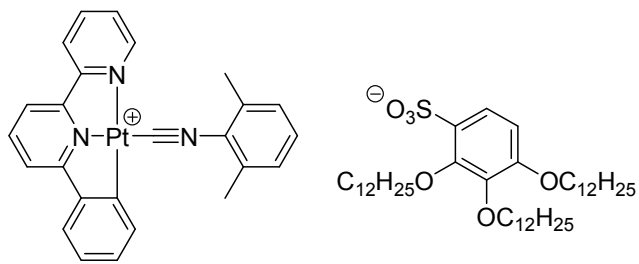
All starting materials were purchased from commercial sources and used as received. The solvents used for synthesis were of analytical grade unless stated otherwise. The solvents used for nanostructure preparations and photophysical measurements were of HPLC grade. The compounds **1**·Cl–**3**·Cl,<sup>1</sup> **4**·Cl<sup>2</sup> and Na·**A**<sup>3</sup> were prepared according to literature methods.

Electron-spray ionization (ESI) mass spectra were obtained on a Finnigan MAT 95 mass spectrometer. <sup>1</sup>H NMR spectra were recorded with Bruker DRX 300 or Avance 400 FT-NMR spectrometers. Elemental analyses were performed by Beijing Institute of Chemistry, Chinese Academy of Sciences. Infrared spectra were recorded on a Bio-Rad FT-IR spectrometer. UV-vis absorption spectra were recorded on a Perkin-Elmer Lambda 19 UV/vis spectrophotometer. Steady-state emission spectra were obtained on a SPEX 1681 Fluorolog-2 series F111AI fluorescence spectrophotometer. Emission lifetime measurements were performed with a Quanta Ray DCR-3 pulsed Nd:YAG laser system (pulse output 355 nm, 8 ns). Luminescent quantum yields were referenced to degassed [Ru(bpy)<sub>3</sub>](ClO<sub>4</sub>)<sub>2</sub> in acetonitrile ( $\Phi_r = 0.062$ ) with estimated error of  $\pm 15\%$ .

TEM and SAED were performed on a Philips Tecnai G2 20 S-TWIN transmission electron microscope with an accelerating voltage of 200 kV. The TEM micrographs were taken by Gatan MultiScan Camera Model 794. TEM samples were prepared by depositing a few drops of dispersion on the formvar-coated copper grids and the excess solvent was removed by a piece of filter paper. The SEM images were taken on a Hitachi S-4800 field emission scanning electron microscope operating at 3.0 kV. SEM samples were prepared by drop-casting suspensions onto silicon wafers. No gold or platinum sputtering was applied before SEM observations.

The powder XRD patterns were recorded on a Bruker D8 Powder X-ray Diffractometer operating with graphite monochromatized CuK<sub>α</sub> radiation ( $\lambda = 1.54056 \text{ \AA}$ ) and a nickel filter.

- 
- (1) W. Lu, Y. Chen, V. A. L. Roy, S. S. Y. Chui and C. M. Che, *Angew. Chem. Int. Ed.*, 2009, **48**, 7621–7625.
  - (2) N. A. Larew, A. R. Van Wassen, K. E. Wetzel, M. M. Machala and S. D. Cummings, *Inorg. Chim. Acta*, 2010, **363**, 57–62.
  - (3) U. Beginn, L. L. Yan, S. N. Chvalun, M. A. Shcherbina, A. Bakirov and M. Moller, *Liq. Cryst.*, 2008, **35**, 1073–1093.



**1·A:** MS (ESI): m/z 557.3 [M<sup>+</sup>]; 709.9 [M<sup>-</sup>]. <sup>1</sup>H NMR (400 MHz, CDCl<sub>3</sub>): δ 9.18 (d, 1H, J = 8.1 Hz), 8.84 (d, 1H, J = 7.9 Hz), 8.66 (d, 1H, J = 5.3 Hz), 8.40 (t, 1H, J = 7.9 Hz), 8.14 (t, 1H, J = 8.1 Hz), 7.74–7.71 (m, 2H), 7.65 (d, 1H, J = 7.9 Hz), 7.43–7.31 (m, 3H), 7.24 (d, 2H, J = 7.8 Hz), 7.15–7.06 (m, 2H), 6.55 (d, 1H, J = 8.8 Hz), 4.23 (t, 2H, J = 7.2 Hz), 3.96 (t, 4H, J = 6.5 Hz), 2.57 (s, 6H), 1.86–1.71 (m, 6H), 1.48–1.18 (m, 54H), 0.90–0.83 (m, 9H). Elemental analysis Calcd for C<sub>67</sub>H<sub>97</sub>N<sub>3</sub>O<sub>6</sub>PtS: C, 63.48; H, 7.71; N, 3.31. Found: C, 63.20; H, 7.76; N, 3.25.

medium (T / K)	$\lambda_{\text{abs}}$ / nm (ε / mol <sup>-1</sup> dm <sup>3</sup> cm <sup>-1</sup> )	$\lambda_{\text{em}}$ / nm (τ / μs)	ϕ
CH <sub>2</sub> Cl <sub>2</sub> (298)	240 (28600)	530 (1.6)	0.03
	270 (sh, 22670)		
	334 (10390)		
	350 (sh, 9330)		
	400 (sh, 490)		
Cyclohexane (298)	267 (sh, 23260)	673(0.9)	0.06
	329 (9860)		
	431 (2020)		
2-MeTHF (77)		715(3.4)	
Solid (298)		678(0.5)	
Solid (77)		758(1.6)	

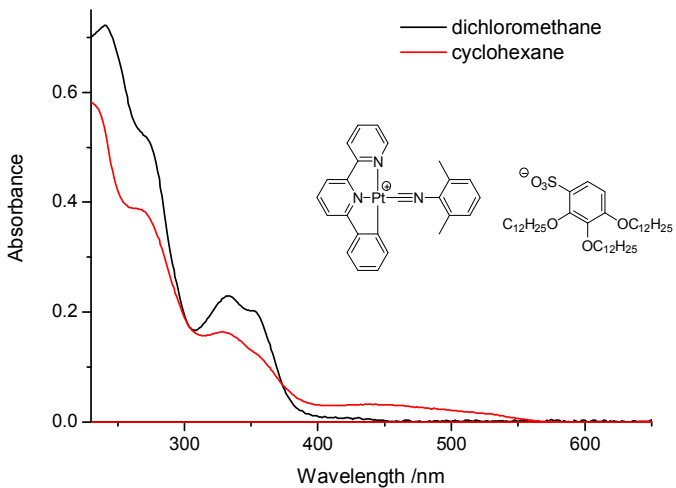


**Fig. S1** UV-vis absorption spectra of **1-A** in dichloromethane (black line) and cyclohexane (red line).

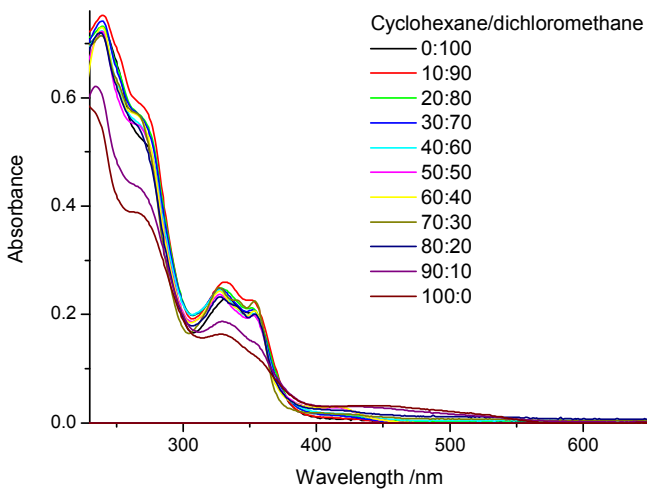


**Fig. S2** UV-vis absorption spectra of **1-A** in cyclohexane/dichloromethane with v/v from 0:100 to 100:0 (concentration  $\sim 2.0 \times 10^{-5}$  mol dm $^{-3}$ ).

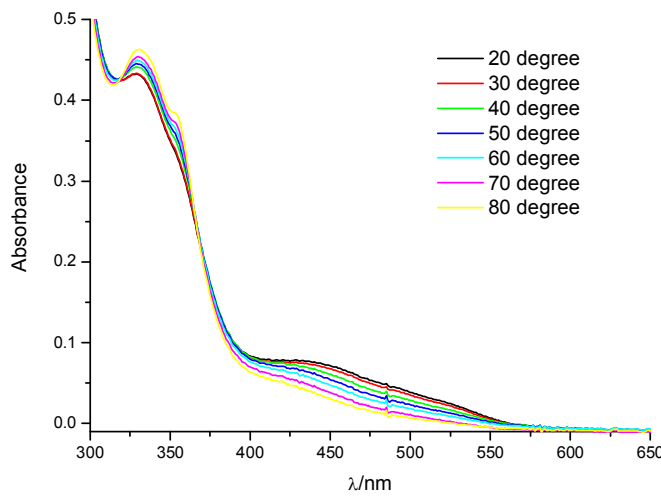


**Fig. S3** UV-vis absorption traces of **1·A** in decalin (concentration  $\sim 5.0 \times 10^{-5} \text{ mol dm}^{-3}$ ) when temperature increases from 20 to 80 °C.

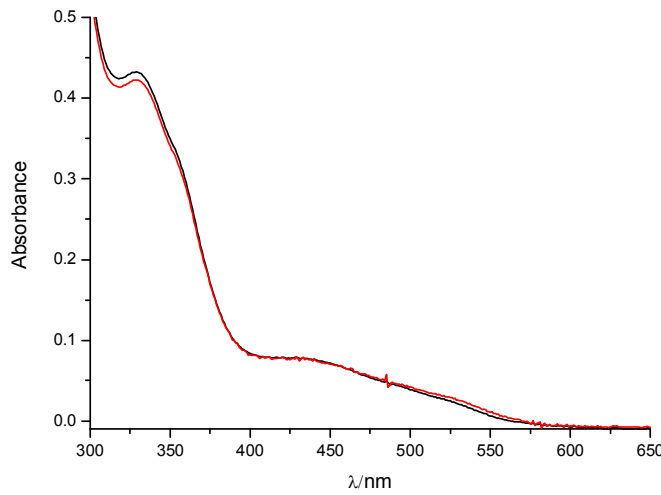


**Fig. S4** UV-vis absorption spectra of **1·A** in decalin at 20 °C before (black line) and after (red line) variable temperature experiments.

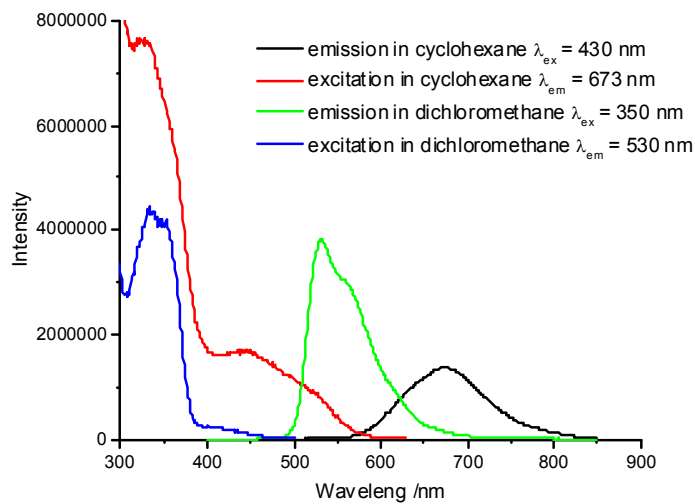


**Fig. S5** Emission and excitation spectra of **1-A** in dichloromethane and cyclohexane solution (concentration  $\sim 2.0 \times 10^{-5} \text{ mol dm}^{-3}$ ).

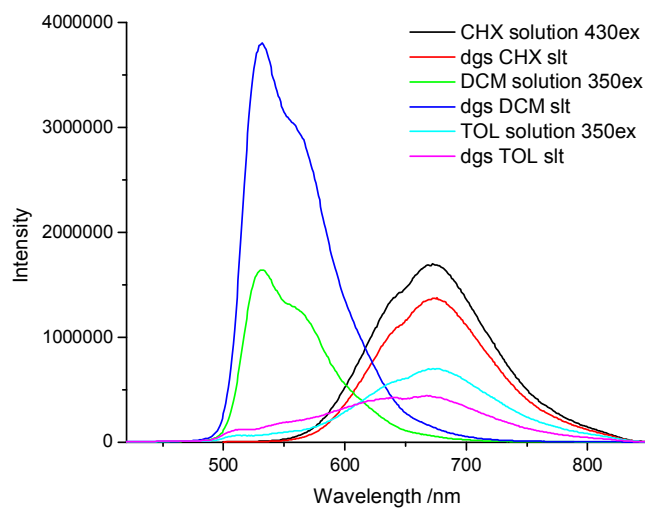


**Fig. S6** Emission spectra of **1-A** in varying solvent systems.

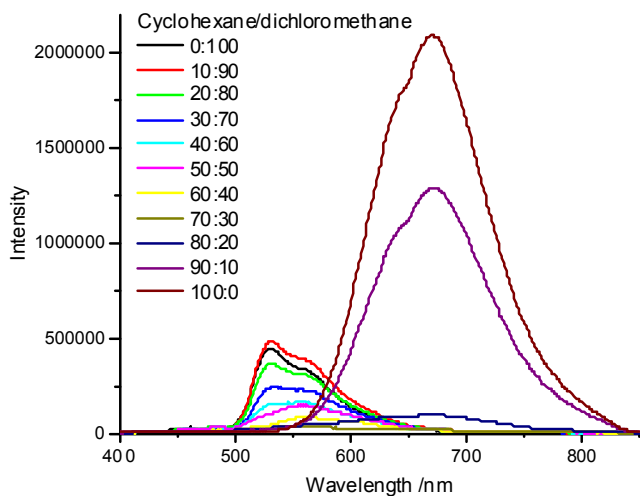


**Fig. S7** Spectroscopic trances for **1-A** in cyclohexane/dichloromethane with v/v from 0:100 to 100:0 (concentration  $\sim 2.0 \times 10^{-5}$  mol dm $^{-3}$ ) ( $\lambda_{\text{ex}} = 378\text{nm}$ ).

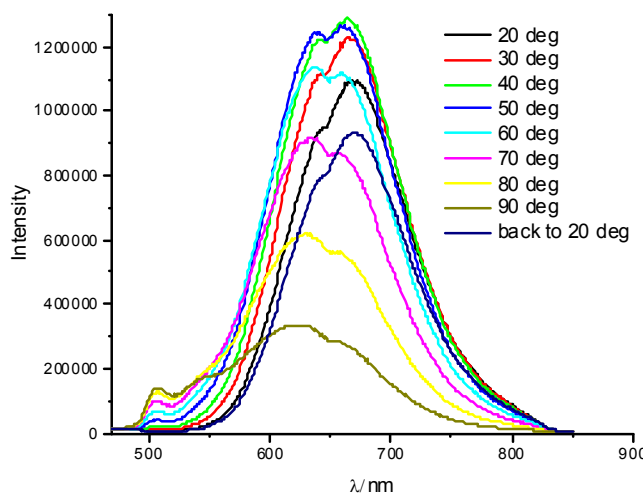


**Fig. S8** Emission spectral traces of **1-A** in decalin (concentration  $\sim 5.0 \times 10^{-5}$  mol dm $^{-3}$ ) when temperature increases from 20 to 90 °C.

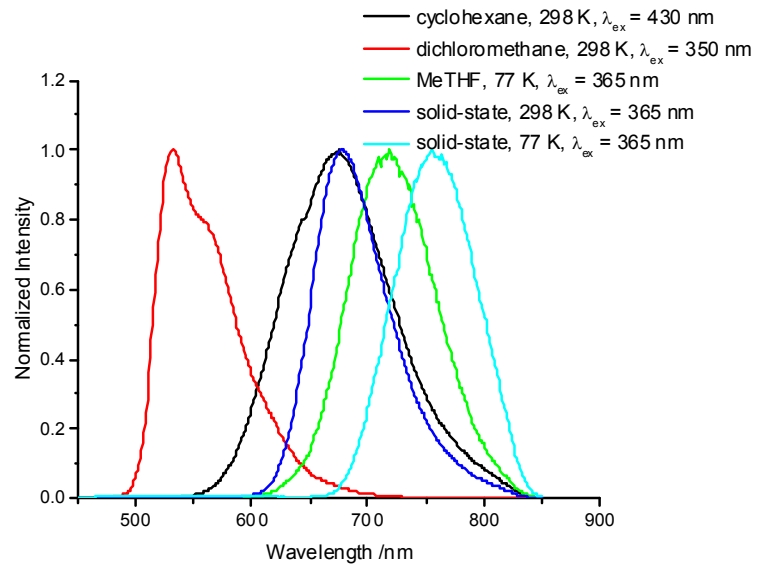
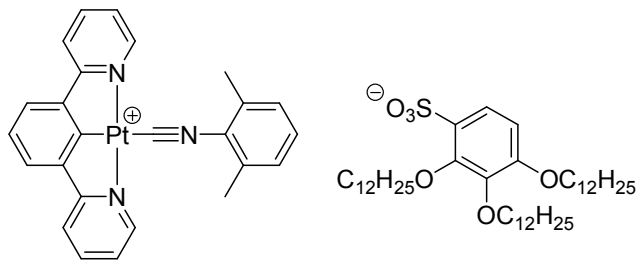


**Fig. S9** Normalized emission spectra of **1·A** in solution and solid state.



**2·A:** MS (ESI): m/z 556.9 [M<sup>+</sup>]; 709.6 [M<sup>-</sup>]. <sup>1</sup>H NMR (400 MHz, CDCl<sub>3</sub>): δ 8.40 (d, 2H, J = 5.6 Hz), 8.14 (t, 2H, 7.8 Hz), 7.81 (d, 2H, J = 8.0 Hz), 7.68 (d, 1H, J = 8.7 Hz), 7.47 (t, 2H, J = 7.3 Hz), 7.42 (d, 2H, J = 7.7 Hz), 7.36 (t, 1H, J = 7.6 Hz), 7.20 (d, 2H, J = 7.6 Hz), 7.09 (t, 1H, J = 7.7 Hz), 6.54 (d, 1H, J = 8.8 Hz), 4.24 (t, 2H, J = 7.1 Hz), 4.00–3.95 (q, 4H), 2.50 (s, 6H), 1.91–1.78 (m, 6H), 1.48–1.19 (m, 54H), 0.90–0.87 (m, 9H). Elemental analysis Calcd for C<sub>67</sub>H<sub>97</sub>N<sub>3</sub>O<sub>6</sub>PtS·H<sub>2</sub>O: C, 62.59; H, 7.76; N, 3.27. Found: C, 62.40; H, 7.56; N, 3.35.

medium (T / K)	$\lambda_{\text{abs}} / \text{nm}$ ( $\epsilon / \text{mol}^{-1}\text{dm}^3\text{cm}^{-1}$ )	$\lambda_{\text{em}} / \text{nm}$ ( $\tau / \mu\text{s}$ )	$\phi$
CH <sub>2</sub> Cl <sub>2</sub> (298)	253 (31860)	490 (6.0)	0.43
	277 (22960)	523 (5.8)	
	288 (27120)		
	317 (8720)		
	332 (15030)		
	351 (5640)		
	400 (sh, 660)		
Cyclohexane (298)	357 (4350)	493 (4.4)	0.36
	383 (4200)	525 (4.2)	
	483 (3710)		
	532 (2370)		
2-MeTHF (77)		486 (7.5)	
		520 (7.0)	
		720 (5.5)	
Solid (298)		628 (0.8)	
Solid (77)		657 (2.0)	

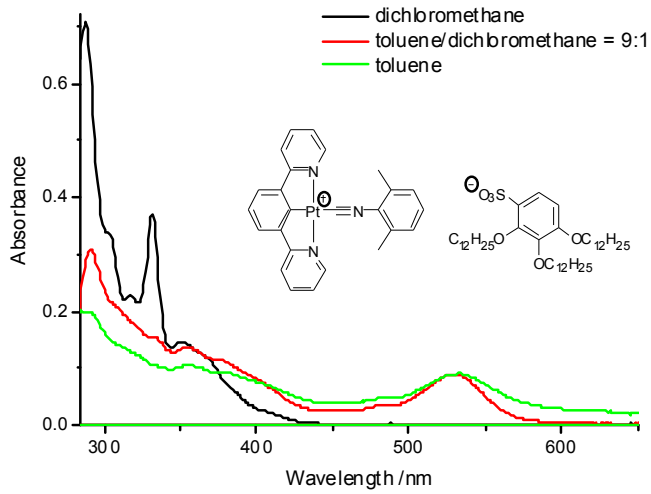


**Fig. S10** UV-vis absorption spectra of **2·A** in dichloromethane (black line), 90% toluene (red line) and pure toluene (green line).

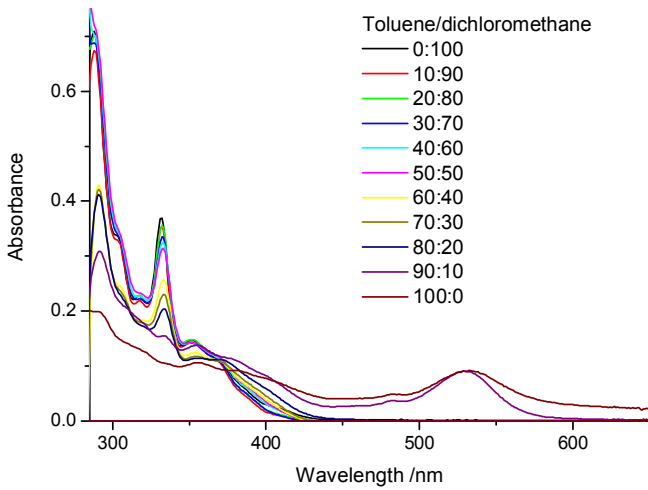


**Fig. S11** UV-vis absorption spectra of **2-A** in toluene/dichloromethane with v/v from 0:100 to 100:0 (concentration  $\sim 2.0 \times 10^{-5}$  mol dm $^{-3}$ ).

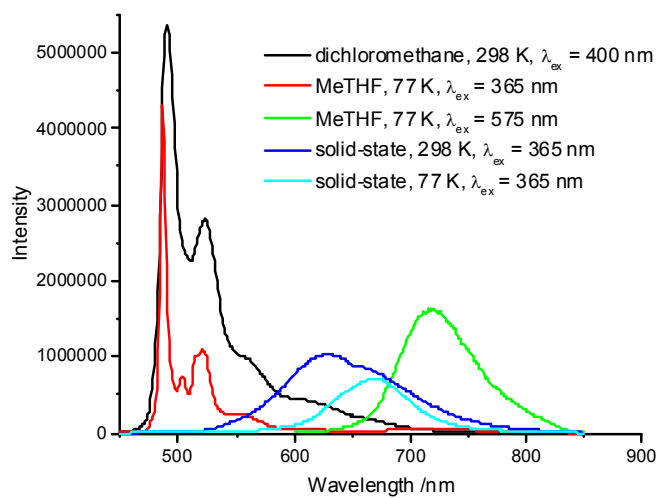


**Fig. S12** Emission spectra of **2·A** in solution and solid state.

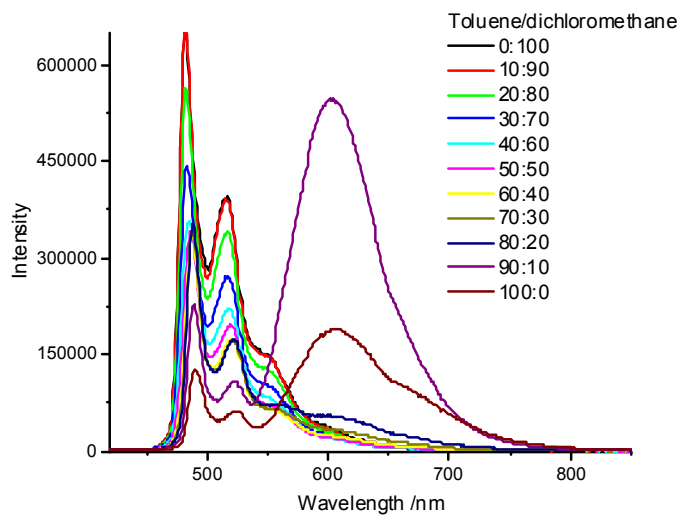


**Fig. S13** Spectroscopic traces for **2·A** in toluene/dichloromethane with v/v from 0:100 to 100:0 (concentration  $\sim 2.0 \times 10^{-5} \text{ mol dm}^{-3}$ ) ( $\lambda_{\text{ex}} = 370 \text{ nm}$ ).

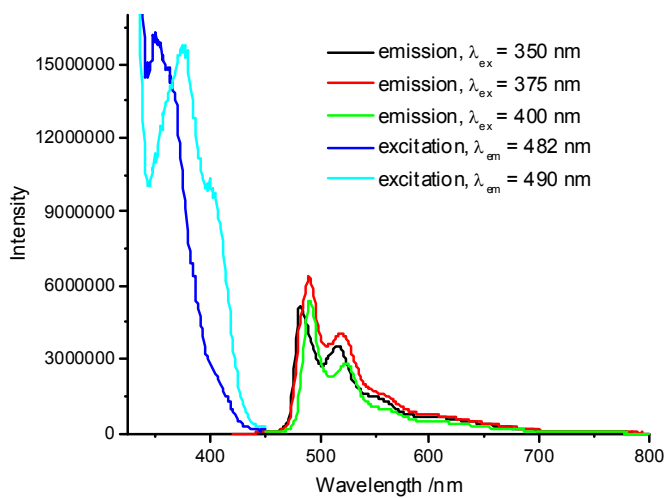


**Fig. S14** Emission spectra of **2·A** in degassed dichloromethane solution with varying excitation wavelength.

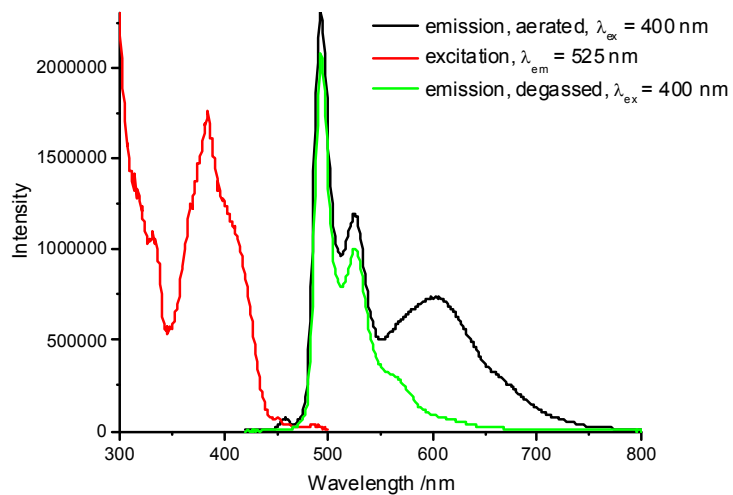


**Fig. S15** Emission and excitation spectra of **2·A** in toluene solution.

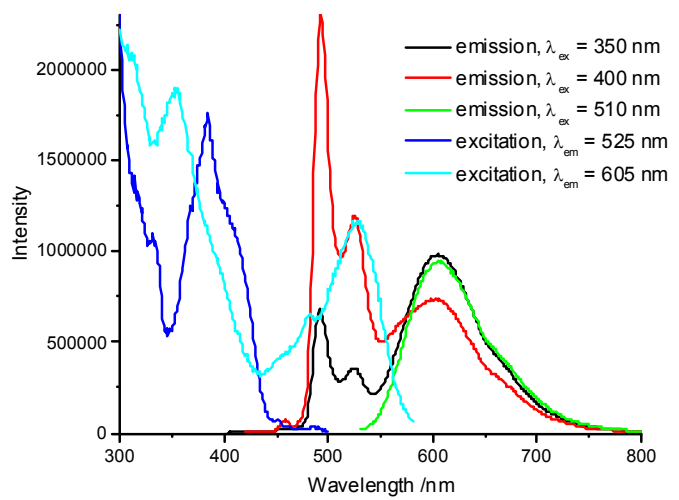
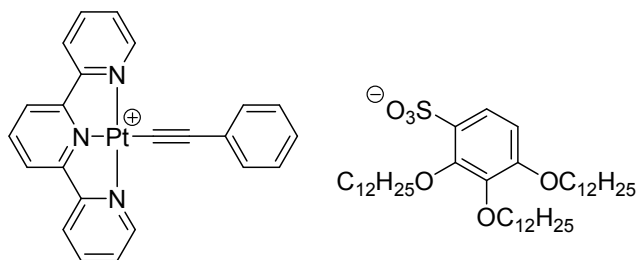


**Fig. S16** Emission spectra of **2·A** in an aerated toluene solution with varying excitation wavelength.



**3·A:** MS (ESI): m/z 529.1 [M<sup>+</sup>]; 709.6 [M<sup>-</sup>]. <sup>1</sup>H NMR (400 MHz, CDCl<sub>3</sub>): δ 8.88 (d, 2H, J = 4.8 Hz), 8.66–8.60 (m, 4H), 8.18–8.10 (m, 3H), 7.78 (d, 1H, J = 8.7 Hz), 7.53 (t, 2H, J = 6.3 Hz), 7.38 (d, 2H, J = 7.6 Hz), 7.32–7.28 (m, 3H), 6.67 (d, 1H, J = 8.8 Hz), 4.28 (t, 2H, J = 7.0 Hz), 4.02–3.98 (q, 4H), 1.89–1.75 (m, 6H), 1.47–1.16 (m, 54H), 0.90–0.82 (m, 9H). Elemental analysis Calcd for C<sub>65</sub>H<sub>93</sub>N<sub>3</sub>O<sub>6</sub>PtS·H<sub>2</sub>O·CH<sub>2</sub>Cl<sub>2</sub>: C, 59.04; H, 7.28; N, 3.13. Found: C, 58.84; H, 7.16; N, 3.31.

medium (T / K)	$\lambda_{\text{abs}}$ / nm ( $\varepsilon$ / mol <sup>-1</sup> dm <sup>3</sup> cm <sup>-1</sup> )	$\lambda_{\text{em}}$ / nm ( $\tau$ / $\mu$ s)	$\phi$
CH <sub>2</sub> Cl <sub>2</sub> (298)	242 (22110) 284 (sh, 12170) 316 (6730) 332 (6170) 346 (6370) 460 (1770)	609 (1.0)	0.02
Cyclohexane (298)	238 (36010) 267 (sh, 26650) 331 (7770) 480 (3580)	Non-emissive	
2-MeTHF (77)		694 (0.9)	
Solid (298)		688 (0.2)	
Solid (77)		701 (1.1)	

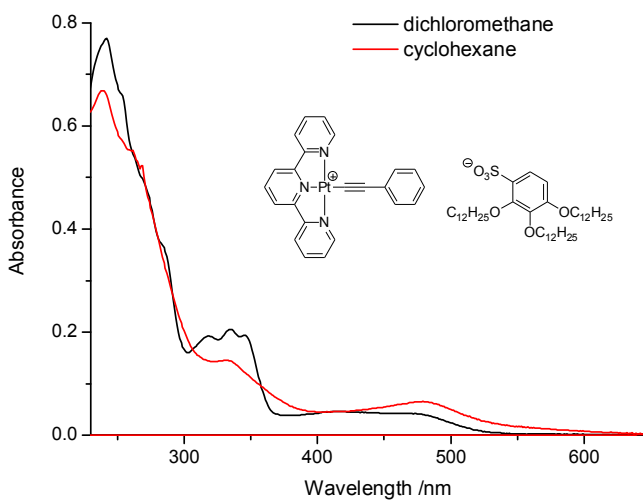


**Fig. S17** UV-vis absorption spectra of **3-A** in dichloromethane (black line) and cyclohexane (red line).

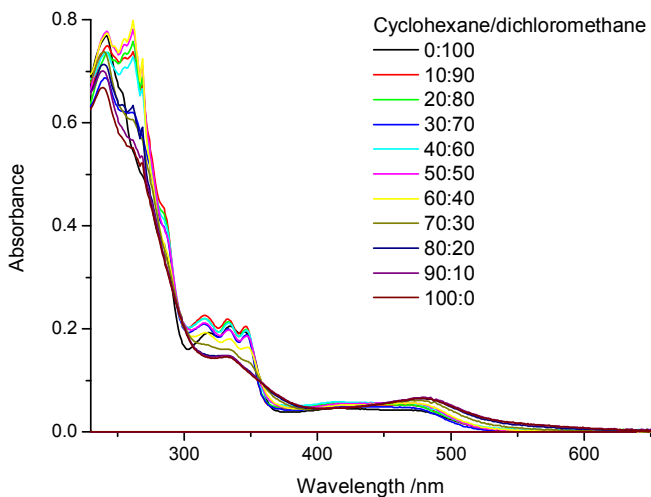


**Fig. S18** UV-vis absorption spectra of **3-A** in cyclohexane/dichloromethane with v/v from 0:100 to 100:0 (concentration  $\sim 2.0 \times 10^{-5}$  mol dm $^{-3}$ ).

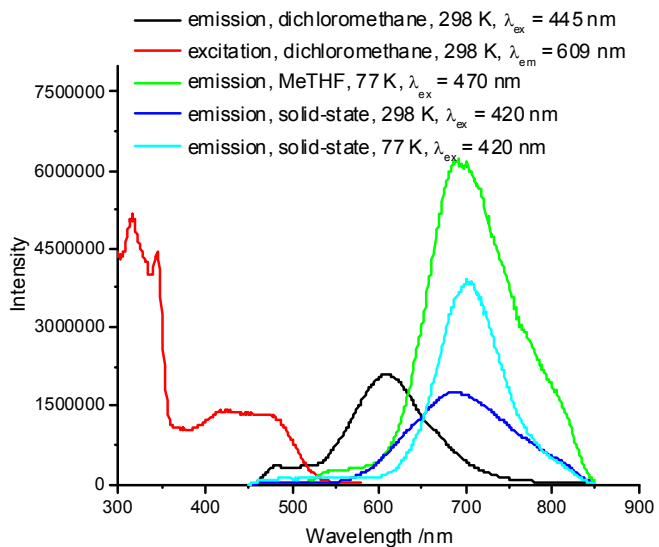


**Fig. S19** Emission and excitation spectra of **3·A** in solution and solid state.

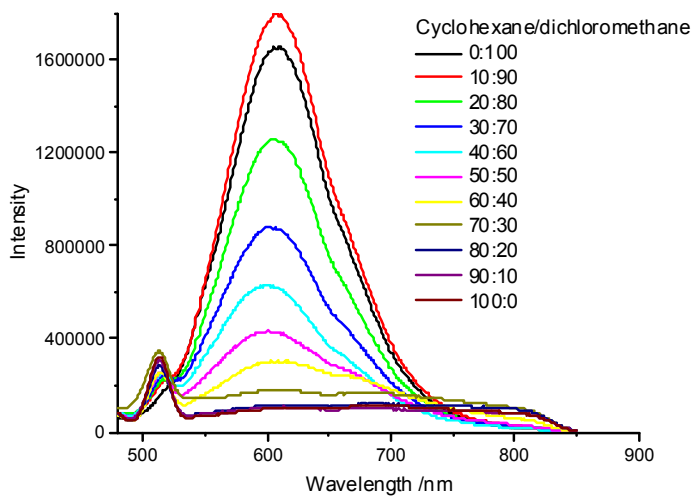
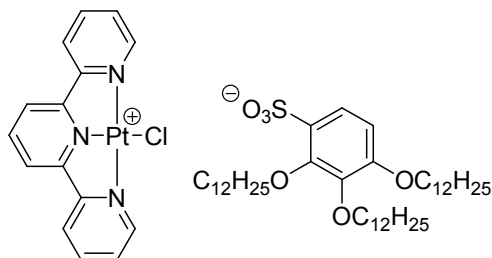


**Fig. S20** Spectroscopic trances for **3·A** in cyclohexane/dichloromethane with v/v from 0:100 to 100:0 (concentration  $\sim 2.0 \times 10^{-5} \text{ mol dm}^{-3}$ ) ( $\lambda_{\text{ex}} = 445 \text{ nm}$ ).



**4·A:** MS (ESI): m/z 463.1 [M<sup>+</sup>]; 710.0 [M<sup>-</sup>]. <sup>1</sup>H NMR (400 MHz, CDCl<sub>3</sub>): δ 8.90 (d, 2H, J = 8.2 Hz), 8.84 (d, 4H, J = 7.5 Hz), 8.34 (t, 1H, J = 8.1 Hz), 8.19 (t, 2H, J = 8.0 Hz), 7.76 (d, 1H, J = 8.7 Hz), 7.68 (t, 2H, J = 6.9 Hz), 6.66 (d, 1H, J = 8.8 Hz), 4.26 (t, 2H, J = 7.0 Hz), 4.01–3.96 (q, 4H), 1.84–1.73 (m, 6H), 1.47–1.15 (m, 54H), 0.90–0.83 (m, 9H). Elemental analysis Calcd for

$\text{C}_{57}\text{H}_{88}\text{ClN}_3\text{O}_6\text{PtS} \cdot 2\text{H}_2\text{O}$ : C, 56.58; H, 7.66; N, 3.47. Found: C, 56.84; H, 7.50; N, 3.53.

medium (T / K)	$\lambda_{\text{abs}} / \text{nm}$ ( $\epsilon / \text{mol}^{-1}\text{dm}^3\text{cm}^{-1}$ )	$\lambda_{\text{em}} / \text{nm}$ ( $\tau / \mu\text{s}$ )	$\phi$
CH <sub>2</sub> Cl <sub>2</sub> (298)	258 (19630)	Non-emissive	
	284 (19180)		
	308 (11250)		
	321 (7850)		
	335 (7450)		
	352 (5290)		
	383 (1680)		
	400 (1550)		
Cyclohexane (298)	256 (23850)	630 (0.5)	0.04
	282 (sh, 18380)	660 (0.5)	
	333 (10030)		
	487 (1680)		
2-MeTHF (77)		628 (4.0)	
Solid (298)		640 (0.3)	
		660 (0.3)	
Solid (77)		642 (2.5)	

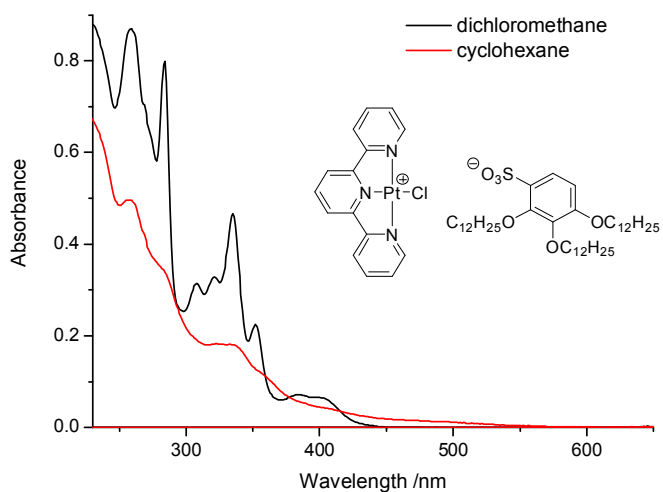


**Fig. S21** UV-vis absorption spectra of **4-A** in dichloromethane (black line) and cyclohexane (red line).

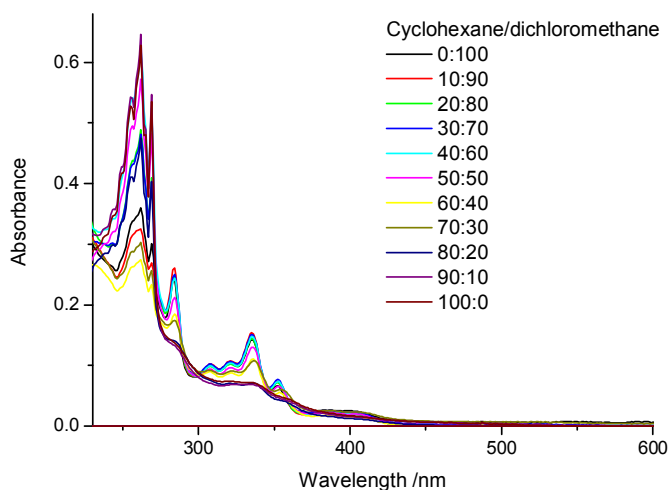


**Fig. S22** UV-vis absorption spectra of **4-A** in cyclohexane/dichloromethane with v/v from 0:100 to 100:0 (concentration  $\sim 2.0 \times 10^{-5}$  mol dm $^{-3}$ ).

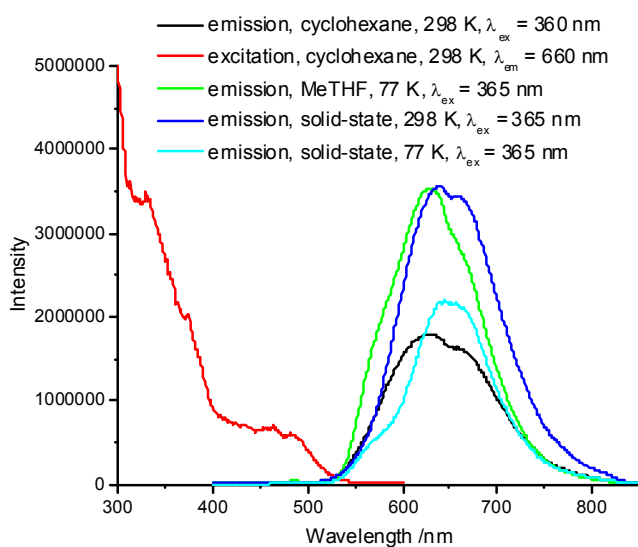


**Fig. S23** Emission and excitation spectra of **4·A** in solution and solid state.

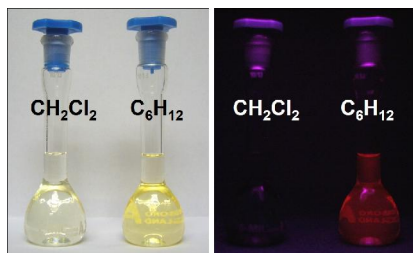
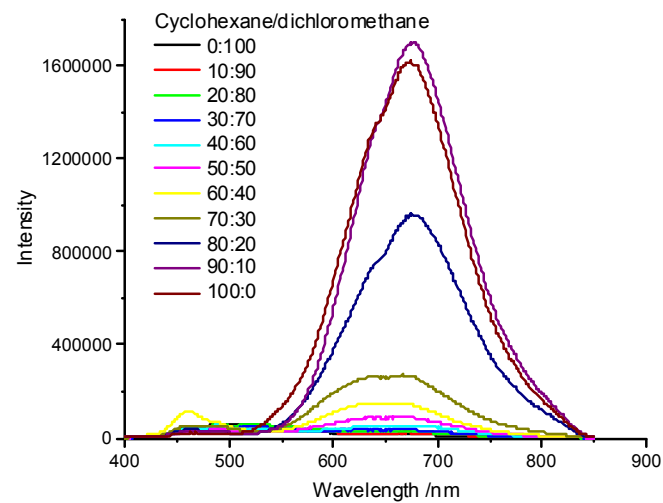


**Fig. S24** Spectroscopic trances for **4·A** in cyclohexane/dichloromethane with v/v from 0:100 to 100:0 (concentration  $\sim 2.0 \times 10^{-5}$  mol dm $^{-3}$ ) ( $\lambda_{ex} = 358$  nm).

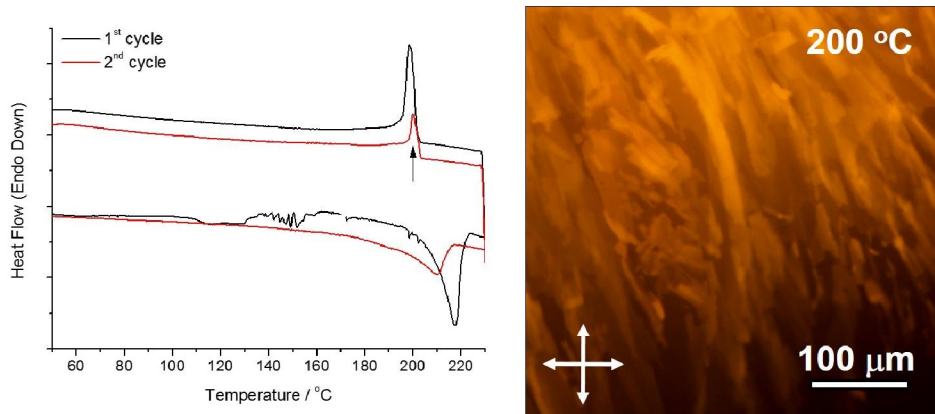


**Fig. S25** DSC thermograms of **2·A** and optical textures of **2·A** between two crossed polarizers.

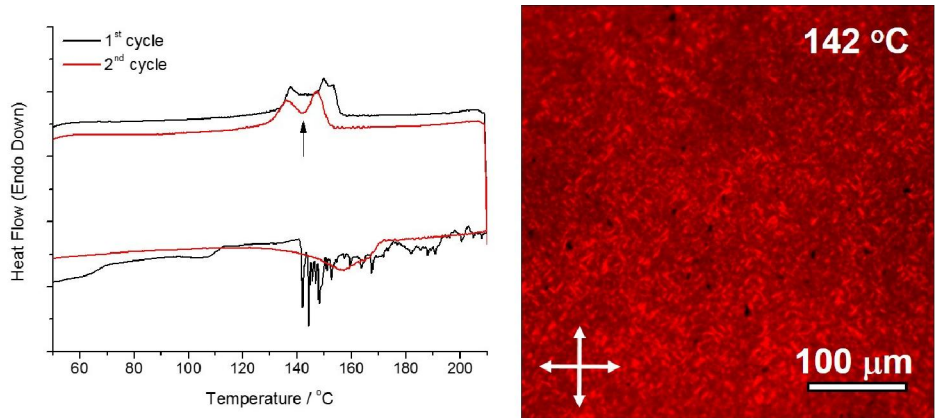


**Fig. S26** DSC thermograms of **3·A** and optical textures of **3·A** between two crossed polarizers.

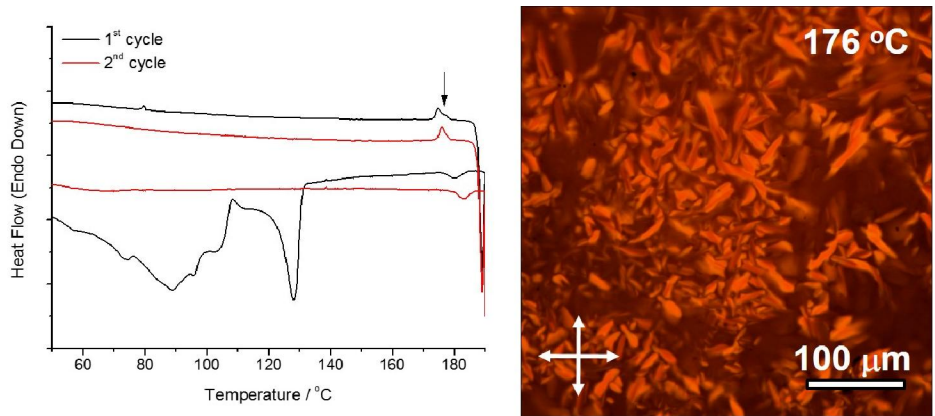


**Fig. S27** DSC thermograms of **4·A** and optical textures of **4·A** between two crossed polarizers.

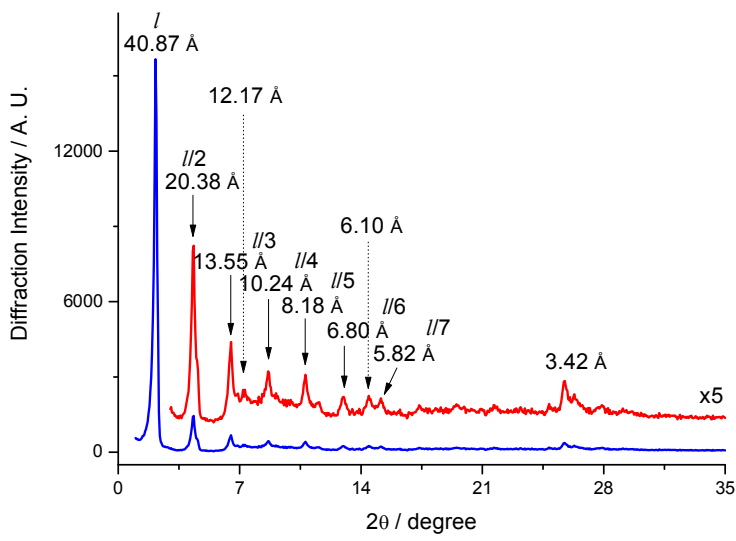


**Fig. S28** XRD diffraction pattern of **2·A** at 25 °C.

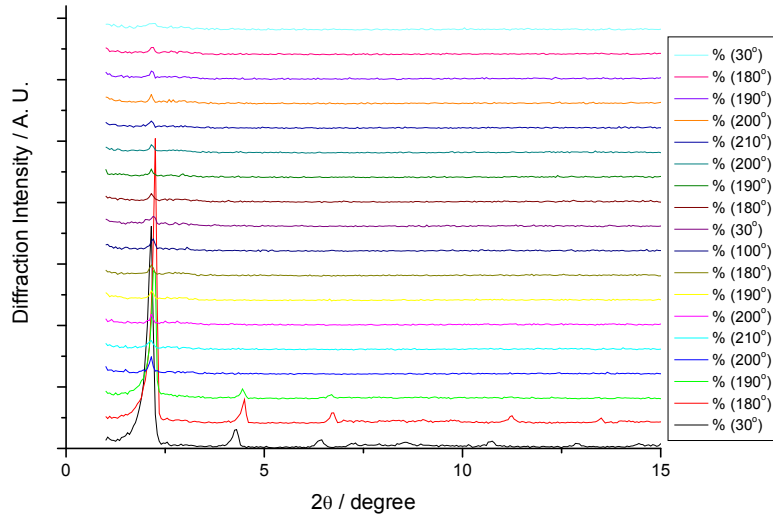


**Fig. S29** Variable-temperature XRD diffraction pattern of **2·A** in the low-angle region.

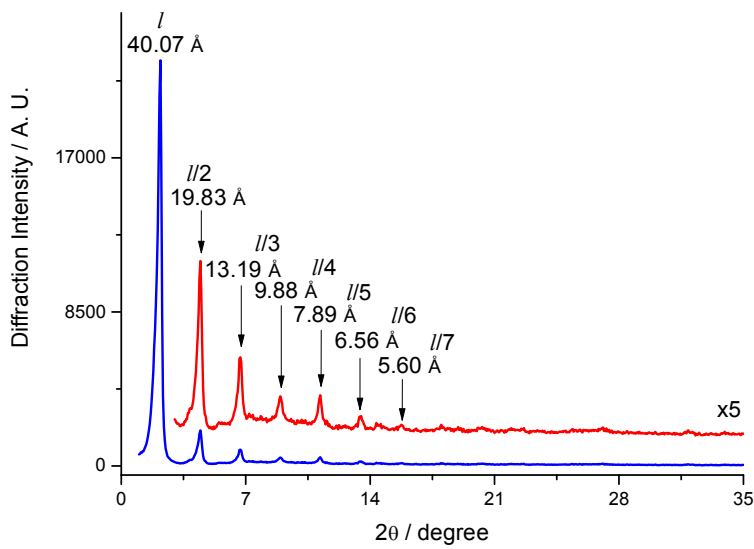


**Fig. S30** XRD diffraction pattern of **3·A** at 25 °C.

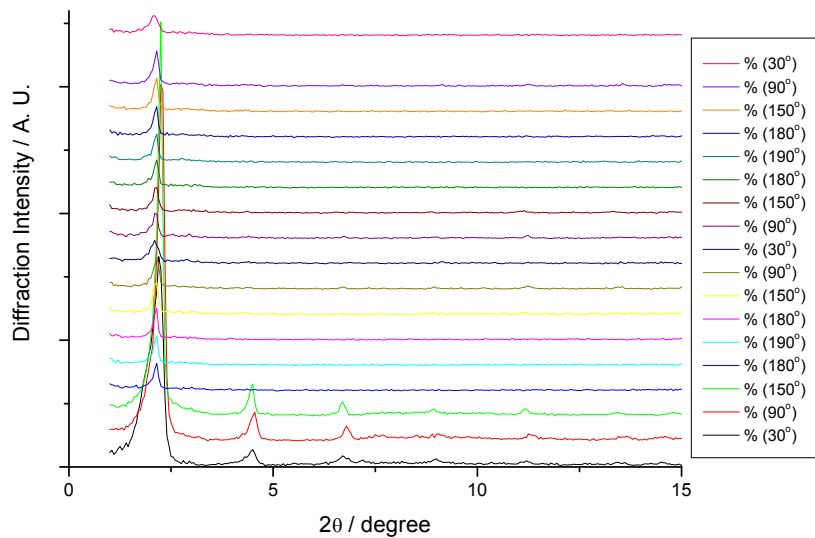


**Fig. S31** Variable-temperature XRD diffraction pattern of **3·A** in the low-angle region.

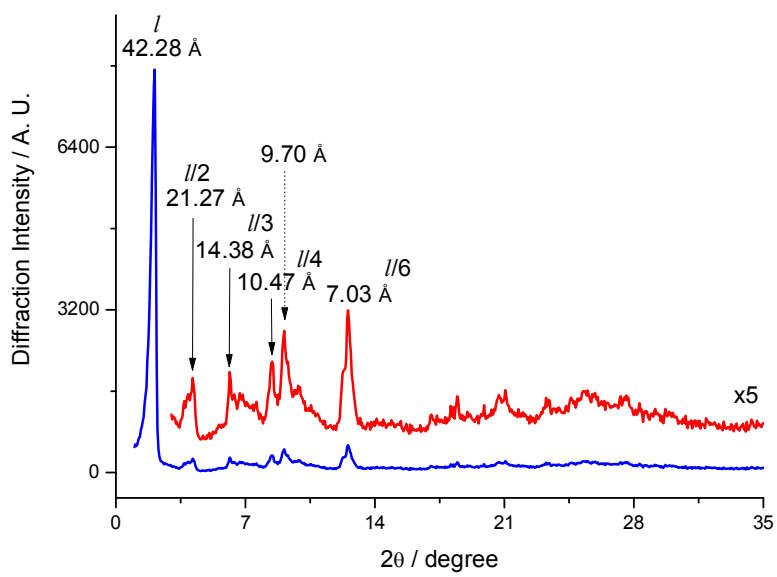


**Fig.**

**S32** XRD diffraction pattern of **4·A** at 25 °C.

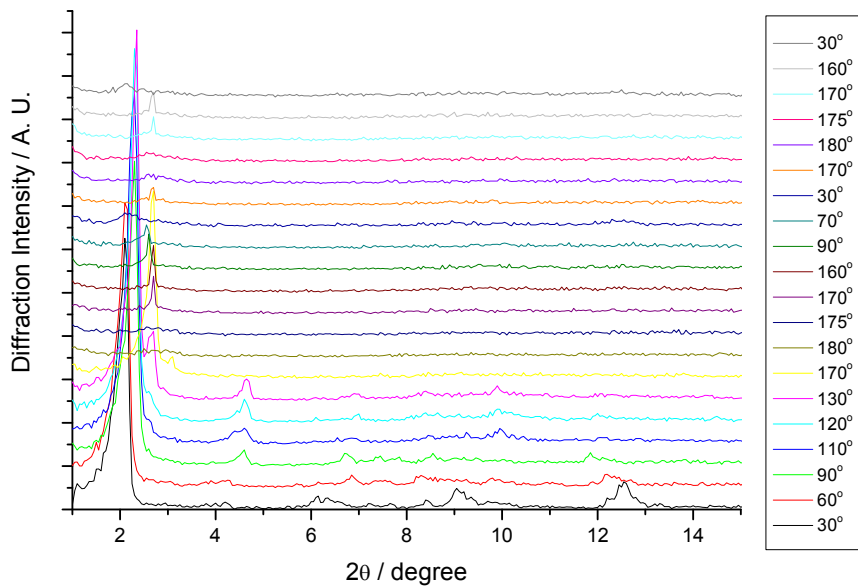


**Fig. S33** Variable-temperature XRD diffraction pattern of **4·A** in the low-angle region.